



The multi-innovation extended Kalman filter algorithm for battery SOC estimation

Wenqian Li¹ · Yan Yang¹ · Dongqing Wang¹ · Shengqiang Yin²

Received: 8 June 2020 / Revised: 24 July 2020 / Accepted: 25 July 2020 / Published online: 21 August 2020
© Springer-Verlag GmbH Germany, part of Springer Nature 2020

Abstract

For a lithium battery, a second-order equivalent circuit model is adopted by studying the battery characteristic, and a state space equation with state of charge (SOC) being one state is constructed. To promote the SOC estimation precision of the extended Kalman filter (EKF) method for a lithium battery, this paper explores a multi-innovation extended Kalman filter (MI-EKF) algorithm to estimate the battery SOC by expanding a single innovation at current instant to multi-innovations containing information from current and previous instants. The aim is to increase the amount of information, and to get the more accurate estimated SOC. In addition, based on the battery difference equation, a stochastic gradient algorithm with a forgetting factor (FFSG) is used to identify the battery parameters. Finally, a lithium battery test bench is set up to sample charge-discharge data and to implement MATLAB simulation experiment; the experiment results confirm that the MI-EKF algorithm can accurately and effectively estimate the battery SOC.

Keywords Lithium battery · State of charge (SOC) · Multi-innovation · Extended Kalman filter

Introduction

The research for battery performance reflects in several aspects [1–4]. Among them, the SOC estimation is one of research hotspots due to its accurate prediction deciding the effective use of battery and playing a vital role in the battery management system.

The SOC estimation methods

The general classification for SOC estimation

Due to SOC being unable directly measured, it can only be computed by using the battery operating voltage and current [5–8], etc. At present, well-known methods for SOC estimation include the following:

- The traditional SOC estimation methods contain the ampere-hour (AH) integration method [9] and the OCV method [10–12].
- The data-driven model-based methods [13–19] mainly include the fuzzy logic method [13, 14], the neural network model-based method [15–17], the support vector machine [18], and the difference equation model [19], mostly do not have a physical significance.
- The mechanism model-based SOC estimation methods [20, 21] contain the electrochemical model methods [22, 23] and the equivalent circuit model (ECM) methods [24–26], etc.

The comparison of SOC estimation methods

The traditional SOC estimation methods

The traditional methods are simple in theory and easy to implement. However, the AH integration method is difficult to precisely get the initial SOC, and easy to cause cumulative errors. The OCV method must be in the case of a broken circuit, after the battery is rest for a period of time; this requirement makes online measurement impossible.

✉ Dongqing Wang
dqwang64@qdu.edu.cn

¹ College of Electrical Engineering, Qingdao University, Qingdao 266071, China

² Marine Equipment Inspection & Testing Co. Ltd, Qingdao 266071, China

The data-driven model-based methods

The neural network and fuzzy model are two main branches of artificial intelligence [13–17] that belong to the data-driven model-based methods. Their corresponding SOC estimation methods do not rely on accurate battery models, but infer the characteristics or mechanism of the battery by analyzing the sampled input-output data of the battery according to the black-box principle. The disadvantage is that they do not give a clear physical meaning.

The mechanism model-based methods

The mechanism model-based methods continuously catch attentions in the lithium battery modeling field due to the definite physical meaning of the battery model. The electrochemical model is accurate, but the parameters in the model are fairly difficult to obtain.

Among them, the equivalent circuit model (ECM) method is more popular due to its simple and definite physical meaning, and easy to be expressed into a state space equation with SOC being a state [24–26]. In all the SOC estimation methods, the ECM method takes a compromise between model precision and complexity; thus it is the most appropriate SOC online estimation technique.

The ECM-based Kalman filter (KF) method

The Kalman filter is the mainstream mean to solve state estimation with SOC being one state in a state space equation formed from the ECM. The basic KF method is a popular linear state identification technique which recursively estimates the state of a linear state space equation by seeking the minimum of the mean square error between the practical state and the optimal estimated state [27, 28]. Because the process and measurement models of the lithium battery are nonlinear functions, the linear KF does not suitable; the extension of a linear KF algorithm becomes necessary.

The extended Kalman filter (EKF) algorithm

The EKF is a well-known nonlinear version of the linear KF algorithm [29]; it adopts the linearization method of the nonlinear function which takes the Taylor expansion to approximate the battery nonlinear function into a linear function [30–32], so as to use the KF algorithm to estimate the battery SOC [33]. The limitation is that the error caused by taking the first-order in the Taylor expansion would accumulate with the recursion increasing. The drawback of ignoring higher order terms in Taylor expansion leads to the search of a novel EKF technique. The adaptive EKF algorithm adaptively updates the covariance matrices in Kalman filter estimation method

[34]. In addition, the robust EKF could effectively promote the SOC estimation precision caused by the error from incorrect initial SOC values [35].

The unscented Kalman filter (UKF) algorithm

Different from the EKF algorithm, the UKF adopts the unscented transformation (UT) for linearization, introduces sigma points to catch the state posterior mean and covariance without using Taylor expansion for the linearization of the nonlinear battery equation [36–39], and achieves the precision of second-order Taylor series expansion. Huang et al. evaluated the performance between the EKF and the UKF algorithms [29] to verify the high precision and fast convergence speed of the UKF algorithm. He et al. used the self-adjust UKF to compute the SOC with high precision [40]. But the EKF and UKF algorithms exist problems of dimensionality and divergence. To adapt the high-dimensional state estimation, Arasaratnam et al. presented the cubature Kalman filter technique in 2010 [41].

The cubature Kalman filter (CKF) algorithm

By adopting the radial-spherical cubature rule, the CKF algorithm in SOC estimation is more stable and accurate than the EKF and UKF algorithms [42–44]. In addition, the computation of the CKF is more efficient than that of the UKF, especially for high-dimensional system [45]. The comparison among the CKF, the EKF, and the UKF algorithms is carried out in Ref. [46], with the highest accuracy result of the CKF. To promote the CKF performance, Xia et al. explored an adaptive CKF (ACKF) algorithm to estimate SOC [47], compared it with the CKF and EKF algorithms, and verified that the ACKF is the most accurate and robust against measurement error. But the ACKF needs more computation time than that of the CKF and the EKF.

The dual extended Kalman filter (DEKF) algorithm

The thought of the DEKF is to simultaneously estimate the battery SOC and the equation parameters through two filters [48, 49]. By using a state filter and a parameter filter, the DEKF performs online estimation of the equation states and parameters, so as to overcome the influence of measurement and system noises and to provide superior SOC estimation results [50, 51].

The Kalman filtering method introduces the truncation error in the local linearization process for nonlinear battery systems which causes an increase in the error between the estimated value and the real value. In a strong nonlinear system, the filtering may even cause a divergence phenomenon, which seriously affects the SOC estimation accuracy. Most improved

Kalman filter algorithms promote SOC estimation accuracy to some extent, but still need further improvements.

The estimation influence under noise corruption

The effect of noises on battery parameter identification is much more dominant due to noises often causing the biased battery parameter estimation in some cases. Wei et al. investigated a recursive total least squares (RTLS)-based observer to effectively attenuate the model identification bias caused by noise destruction, and studied an adaptive forgetting RTLS to compensate the influence of noise and reduce the identification deviation of model parameters [52, 53]. Li et al. explored a bias compensation RLS and EKF co-estimation algorithm for battery SOC estimation under noise corrupted measurements [54].

The Kalman filter type algorithms usually are unbiased. As described in [55], the smaller the value of noise variances, the smaller the estimation error will be. Zhang et al. adopted the cubature Kalman (CKF) filter algorithm to generate the proposal distribution of the particle filter algorithm order, and used the state and measurement residuals to adaptively adjust the weight of sigma points so as to reduce the influence of noise on the CKF algorithm [56]. He et al. adopted an adaptive extended Kalman filter algorithm to estimate battery SOC by continuously using the observation data to estimate and modify the filter under unknown system noise and the observation noise [57]. Dong et al. studied an adaptive anti-interference extended Kalman filter by using an innovation-based adaptive estimator [32].

The multi-innovation method

The multi-innovation theory is originated in 2007 [58], and is used in gradient identification of a linear regression model. The thought of the multi-innovation theory is to extend a scalar innovation at current instant to an innovation vector with current and previous innovations, so as to enhance the error information and promote the estimation accuracy. This paper investigates the multi-innovation EKF (MI-EKF) algorithm [58–61] to improve the SOC estimation accuracy of the EKF algorithm. The principle is, at each filtering step, to expand the single innovation at current instant to multi-innovations containing information from current and previous instants, to increase the amount of information, and to get the more accurate estimated SOC.

The motivation of this paper is to explore multi-innovation extended Kalman filter (MI-EKF) algorithm to estimate the battery SOC by expanding a single innovation at current instant to multi-innovations containing more information from

current and previous instants. The purpose is to increase the amount of information, and to get the more accurate estimated SOC, so as to decrease the SOC estimation error caused by the Kalman filtering method.

The features of this research list are as follows:

1. For a lithium battery, an equivalent circuit model is adopted by analyzing the battery characteristic, and a state space equation with SOC being one state is constructed.
2. State estimates of the MI-EKF algorithm are corrected by multi-innovations containing current and previous innovations rather than the single innovation at only current instant, which improves the SOC estimation accuracy.
3. Simulation experiment results verify that the MI-EKF algorithm can effectively and accurately compute battery SOC by using data sampling from a lithium battery test device.

This research is arranged as follows. The next section describes the lithium battery circuit, constructs a state space equation for the lithium battery and identifies the battery parameters; Section 3 investigates the MI-EKF-based SOC estimation method; Section 4 sets up an experimental platform to collect data and carry out simulation experiment by using the classical EKF algorithm and the investigated MI-EKF algorithm and analyze the results; Finally, the conclusion is evaluated in Section 5.

The modeling of the battery

This section introduces a suitable battery equivalent circuit and constructs a nonlinear battery state space equation.

The circuit model of the battery

Common battery equivalent circuits have the Thevenin equivalent circuit, the PNGV circuit, the fourth-order dynamic circuit, and the second-order RC circuit [62–64]. This research chooses a second-order RC circuit, which is simple in structure, easy to implement, easy to calculate, and easy to combine with battery estimation algorithms. Refer to Fig. 1; the circuit

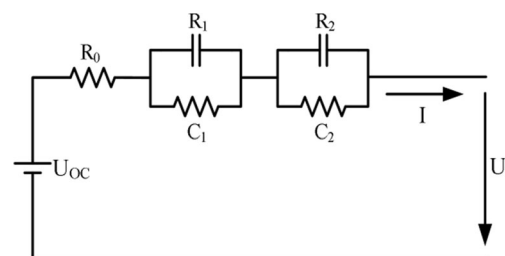


Fig. 1 The battery equivalent circuit

contains U_{OC} , the internal resistance R_0 , and the equivalent resistances R_1C_1 and R_2C_2 . U is the battery terminal voltage, I is the terminal current, and the specified current direction is stipulated as discharge being positive and charge being negative.

According to the Kirchhoff law, the sum of voltage around the entire circuit equals to zero, and then at k instant, we have:

$$U_k = U_{OC,k}(SOC_k) - I_k R_0 - U_k^{R_1 C_1} - U_k^{R_2 C_2} \tag{1}$$

The zero-state voltage responses of the R_1 and R_2 are:

$$\begin{cases} U_{k,zerostate}^{C_1 R_1} = I_{k-1} R_1 \times (1 - \exp(-Ts/\tau_1)) \\ U_{k,zerostate}^{C_2 R_2} = I_{k-1} R_2 \times (1 - \exp(-Ts/\tau_2)) \end{cases} \tag{2}$$

where the time constant are $\tau_1 = R_1 C_1$ and $\tau_2 = R_2 C_2$, respectively; Ts is the sampling period.

The zero-input voltage responses of the R_1 and R_2 are:

$$\begin{cases} U_{k,zeroinput}^{C_1 R_1} = \exp(-Ts/\tau_1) \times U_{k-1}^{C_1 R_1} \\ U_{k,zeroinput}^{C_2 R_2} = \exp(-Ts/\tau_2) \times U_{k-1}^{C_2 R_2} \end{cases} \tag{3}$$

The full voltage responses of the R_1 and R_2 are:

$$\begin{cases} U_k^{C_1 R_1} = U_{k,zerostate}^{C_1 R_1} + U_{k,zeroinput}^{C_1 R_1} \\ = I_{k-1} R_1 \times (1 - \exp(-Ts/\tau_1)) + \exp(-Ts/\tau_1) \times U_{k-1}^{C_1 R_1} \\ U_k^{C_2 R_2} = U_{k,zerostate}^{C_2 R_2} + U_{k,zeroinput}^{C_2 R_2} \\ = I_{k-1} R_2 \times (1 - \exp(-Ts/\tau_2)) + \exp(-Ts/\tau_2) \times U_{k-1}^{C_2 R_2} \end{cases} \tag{4}$$

Circuit parameter estimation

The stochastic gradient algorithm with forgetting factor (FFSG) is used to identify the battery parameters. The parameters to be identified include R_0, R_1, R_2, C_1, C_2 . The transfer function of the system can be obtained from Fig. 1:

$$\begin{aligned} G(S) &= \frac{U(S)}{I(S)} = \frac{U_{OC}(S) - U_L(S)}{I(S)} \\ &= R_0 + \frac{R_1}{1 + R_1 C_1 S} + \frac{R_2}{1 + R_2 C_2 S} \end{aligned} \tag{5}$$

Using bilinear transformation to discretize continuous functions, let:

$$S = \frac{2(1 - Z^{-1})}{T(1 + Z^{-1})} \tag{6}$$

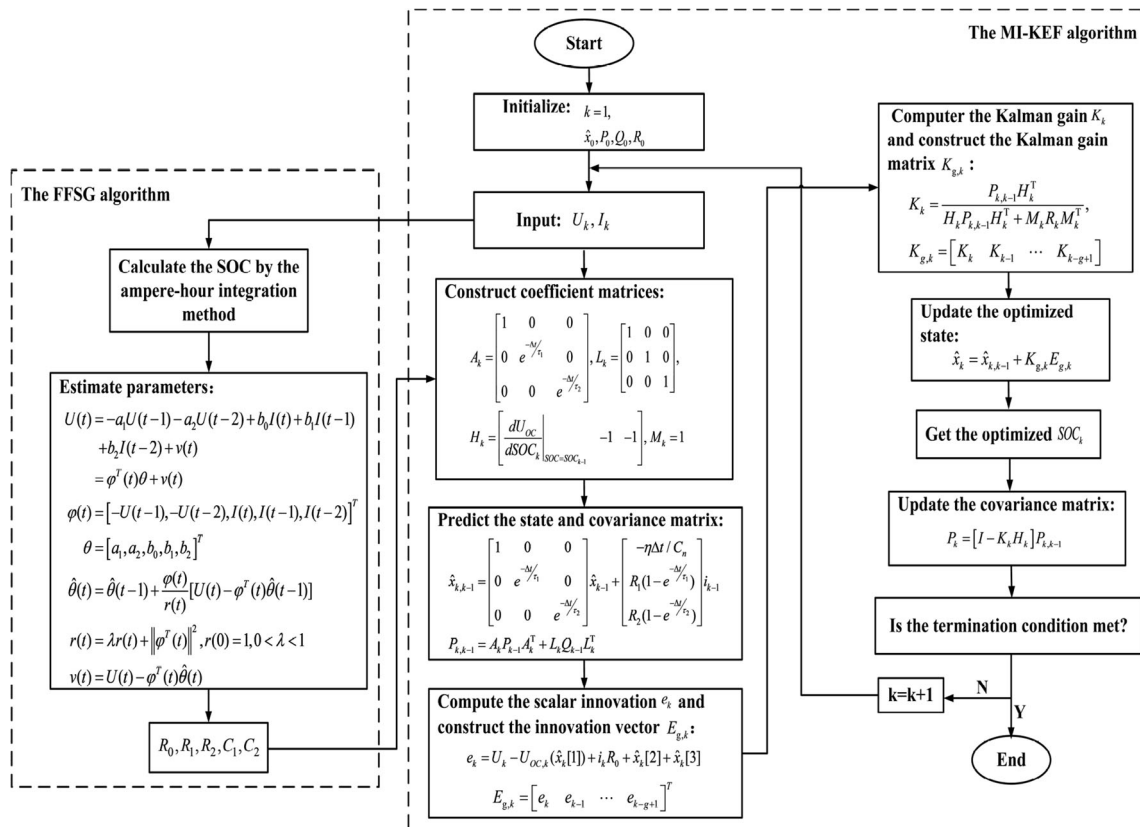


Fig. 2 The procedures of the MI-EKF algorithm

where T is the sampling period. The transfer function is discretized as:

$$G(Z) = \frac{U(Z)}{I(Z)} = \frac{b_0 + b_1Z^{-1} + b_2Z^{-2}}{1 + a_1Z^{-1} + a_2Z^{-2}} \tag{7}$$

where:

$$\left\{ \begin{aligned} a_1 &= \frac{2T^2 - 8\tau_1\tau_2}{(T + 2\tau_1)(T + 2\tau_2)} \\ a_2 &= \frac{(T - 2\tau_1)(T - 2\tau_2)}{(T + 2\tau_1)(T + 2\tau_2)} \\ b_0 &= R_0 + \frac{R_1T}{T + 2\tau_1} + \frac{R_2T}{T + 2\tau_2} \\ b_1 &= \frac{R_0(2T^2 - 8\tau_1\tau_2) + 2(R_1 + R_2)T^2}{(T + 2\tau_1)(T + 2\tau_2)} \\ b_2 &= \frac{R_0(T - 2\tau_1)(T - 2\tau_2) + R_1T(T - 2\tau_2) + R_2T(T - 2\tau_1)}{(T + 2\tau_1)(T + 2\tau_2)} \end{aligned} \right.$$

The corresponding difference equation derived from the discretized transfer function is:

$$U(t) = -a_1U(t-1) - a_2U(t-2) + b_0I(t) + b_1I(t-1) + b_2I(t-2) + v(t) \tag{8}$$

$$= \varphi^T(t)\theta + v(t)$$

where:

1. a_1, a_2, b_0, b_1, b_2 are coefficients to be determined;
2. $\{U(t)\}$ and $\{I(t)\}$ are the output and input sequence of the model respectively;
3. $\{v(t)\}$ is a random noise sequence with zero mean and no correlation.

Let:

$$\varphi(t) = [-U(t-1), -U(t-2), I(t), I(t-1), I(t-2)]^T \tag{9}$$

$$\theta = [a_1, a_2, b_0, b_1, b_2]^T \tag{10}$$

where $\varphi(t)$ is the information vector; θ is the parameter vector.

Then we get the FFSG algorithm as follows [65–68]:

$$\hat{\theta}(t) = \hat{\theta}(t-1) + \frac{\varphi(t)}{r(t)} [U(t) - \varphi^T(t)\hat{\theta}(t-1)] \tag{11}$$

$$r(t) = \lambda r(t-1) + \|\varphi^T(t)\|^2, r(0) = 1, 0 < \lambda < 1 \tag{12}$$

$$v(t) = U(t) - \varphi^T(t)\hat{\theta}(t) \tag{13}$$

where $\hat{\theta}(t)$ represents the estimated parameter vector. By using the FFSG algorithm and the equation (7), we can get the estimates of R_0, R_1, R_2, C_1 and C_2 , shown in Table 1.

Table 1 Parameter estimates of the FFSG algorithm.

R_0	R_1	R_2	C_1	C_2
0.0366 Ω	0.0226 Ω	0.0210 Ω	1575.7F	2815.8 F

The nonlinear battery equation

The circuit model includes three energy storage elements, so the state variable of the lithium battery is set to:

$$x_k = [SOC_k \ U_k^{R_1C_1} \ U_k^{R_2C_2}]^T \tag{14}$$

According to the definition of SOC, we have

$$SOC_k = SOC_{k-1} - \frac{\eta Ts}{C_N} i_{k-1} \tag{15}$$

where

1. η indicates the charge and discharge efficiency, acquired by charge and discharge test. Generally, when charging $\eta = 1$, when discharging $\eta < 1$
2. C_N indicates the rated battery capacity.

From eqs. (4), (14), and (15), the state space equation for a Lithium battery with noises can be written as:

$$x_k = \begin{bmatrix} SOC_k \\ U_k^{R_1C_1} \\ U_k^{R_2C_2} \end{bmatrix} = \begin{bmatrix} 1 & 0 & 0 \\ 0 & e^{-\frac{T}{\tau_1}} & 0 \\ 0 & 0 & e^{-\frac{T}{\tau_2}} \end{bmatrix} \times \begin{bmatrix} SOC_{k-1} \\ U_{k-1}^{R_1C_1} \\ U_{k-1}^{R_2C_2} \end{bmatrix} + \begin{bmatrix} -\eta Ts / C_N \\ R_1 \left(1 - e^{-\frac{T}{\tau_1}}\right) \\ R_2 \left(1 - e^{-\frac{T}{\tau_2}}\right) \end{bmatrix} \times i_{k-1} + w_{k-1} \tag{16}$$

$$U_k = U_{OC,k}(SOC_k) - i_k R_0 - U_k^{R_1C_1} - U_k^{R_2C_2} + v_k \tag{17}$$

where

1. w_{k-1} indicates the system process noise with 0 mean and the covariance matrix Q_{k-1} , i.e., $w_{k-1} \sim (0, Q_{k-1})$
2. v_k indicates the measurement noise with 0 mean and the covariance matrix R_k , i.e., $v_k \sim (0, R_k)$.

Let:

$$f(x_{k-1}, i_{k-1}, w_{k-1}) = \begin{bmatrix} 1 & 0 & 0 \\ 0 & e^{-\frac{T}{\tau_1}} & 0 \\ 0 & 0 & e^{-\frac{T}{\tau_2}} \end{bmatrix} \times x_{k-1} + \begin{bmatrix} -\eta Ts / C_N \\ R_1 \left(1 - e^{-\frac{T}{\tau_1}}\right) \\ R_2 \left(1 - e^{-\frac{T}{\tau_2}}\right) \end{bmatrix} \times i_{k-1} + w_{k-1} \tag{18}$$

$$h(x_k, i_k, v_k) = U_{OC,k}(x_k[1]) - i_k R_0 - x_k[2] - x_k[3] + v_k \quad (19)$$

where $x_k[1] = SOC_k, x_k[2] = U_k^{R_1} C_1, x_k[3] = U_k^{R_2} C_2$.
Then eqs. (18) and (19) can be simply expressed as

$$x_k = f(x_{k-1}, i_{k-1}, w_{k-1}) \quad (20)$$

$$U_k = h(x_k, i_k, v_k) \quad (21)$$

The MI-EKF method for SOC estimation

The classical EKF algorithm

The Taylor expansions of x_k and U_k are, respectively,

$$x_k = f(x_{k-1}, i_{k-1}, w_{k-1}) \approx f(\hat{x}_{k-1}, i_{k-1}, 0) + \left. \frac{\partial f}{\partial x_{k-1}} \right|_{(\hat{x}_{k-1}, i_{k-1}, 0)} (x_{k-1} - \hat{x}_{k-1}) + \left. \frac{\partial f}{\partial w_{k-1}} \right|_{(\hat{x}_{k-1}, i_{k-1}, 0)} w_{k-1} \quad (22)$$

$$U_k = h(x_k, i_k, v_k) \approx h(\hat{x}_k, i_k, 0) + \left. \frac{\partial h}{\partial x_k} \right|_{(\hat{x}_k, i_k, 0)} (x_k - \hat{x}_k) + \left. \frac{\partial h}{\partial v_k} \right|_{(\hat{x}_k, i_k, 0)} v_k \quad (23)$$

According to the EKF principle, Jacobian matrices of $f(\bullet)$ and $h(\bullet)$ are given by:



Fig. 3 The battery test platform

$$A_k = \left. \frac{\partial f(x_{k-1}, i_{k-1}, w_{k-1})}{\partial x_k} \right|_{x_{k-1}=\hat{x}_{k-1}} = \begin{bmatrix} 1 & 0 & 0 \\ 0 & e^{-\frac{\Delta t}{\tau_1}} & 0 \\ 0 & 0 & e^{-\frac{\Delta t}{\tau_2}} \end{bmatrix}$$

$$L_k = \left. \frac{\partial f(x_{k-1}, i_{k-1}, w_{k-1})}{\partial w_{k-1}} \right|_{w_{k-1}=\hat{w}_{k-1}} = \begin{bmatrix} 1 & 0 & 0 \\ 0 & 1 & 0 \\ 0 & 0 & 1 \end{bmatrix}$$

$$H_k = \left. \frac{\partial h(x_k, i_k, v_k)}{\partial x_k} \right|_{x_k=\hat{x}_{k-1}} = \left[\frac{dU_{OC}}{dSOC_k} \right]_{SOC=SOC_{k-1}} \quad -1 \quad -1$$

$$M_k = \left. \frac{\partial h(x_k, i_k, v_k)}{\partial v_k} \right|_{v_k=\hat{v}_k} = 1$$

Fig. 4 The configuration diagram of the battery test system

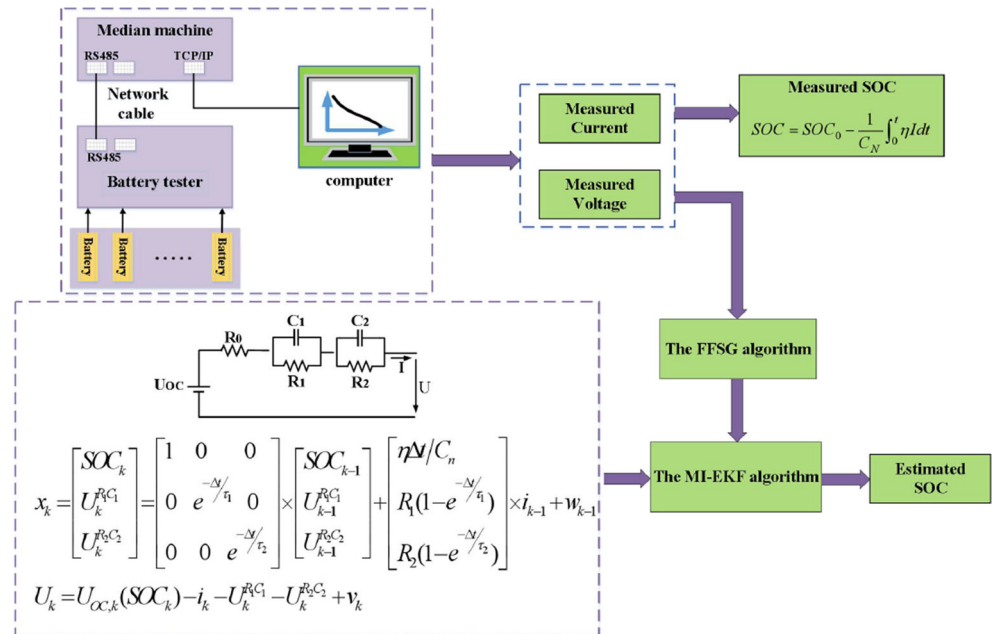


Table 2 General parameters of the battery.

Battery Type	NCR-18650PF
Rated voltage	3.7 V
Operating voltage	2.7 V–4.2 V
Capacitance	2900 mAh + 10%
Rated charge current	1.45A (0.5C)
Max. discharge current	8.7A (3C)

Thus, the EKF algorithm can be expressed as:

$$\hat{x}_{k,k-1} = \begin{bmatrix} 1 & 0 & 0 \\ 0 & e^{-T/\tau_1} & 0 \\ 0 & 0 & e^{-T/\tau_2} \end{bmatrix} \times \hat{x}_{k-1} + \begin{bmatrix} -\eta Ts/C_N \\ R_1(1-e^{-T/\tau_1}) \\ R_2(1-e^{-T/\tau_2}) \end{bmatrix} \times i_{k-1} \quad (24)$$

$$P_{k,k-1} = A_k P_{k-1} A_k^T + L_k Q_{k-1} L_k^T \quad (25)$$

$$K_k = \frac{P_{k,k-1} H_k^T}{H_k P_{k,k-1} H_k^T + M_k R_k M_k^T} \quad (26)$$

$$\hat{x}_k = \hat{x}_{k,k-1} + K_k \{ U_k - U_{OC,k}(\hat{x}_k[1]) + i_k R_0 + \hat{x}_k[2] + \hat{x}_k[3] \} \quad (27)$$

$$P_k = [I - K_k H_k] P_{k,k-1} \quad (28)$$

The investigated MI-EKF algorithm

For nonlinear battery systems, the standard EKF algorithm uses a single innovation to update the state estimates, while the MI-EKF algorithm uses multi-innovations to correct the state estimates, so as to promote the estimation precision [58–61].

The specific approach is to expand the single innovation:

$$e_k = U_k - U_{OC,k}(\hat{x}_k[1]) + i_k R_0 + \hat{x}_k[2] + \hat{x}_k[3] \quad (29)$$

to an innovation vector $E_{g,k}$ (i.e., multi-innovations):

$$E_{g,k} = \begin{bmatrix} e_k \\ e_{k-1} \\ \vdots \\ e_{k-g+1} \end{bmatrix} = \begin{bmatrix} U_k - U_{OC,k}(\hat{x}_k[1]) + i_k R_0 + \hat{x}_k[2] + \hat{x}_k[3] \\ U_{k-1} - U_{OC,k-1}(\hat{x}_{k-1}[1]) + i_{k-1} R_0 + \hat{x}_{k-1}[2] + \hat{x}_{k-1}[3] \\ \vdots \\ U_{k-g+1} - U_{OC,k-g+1}(\hat{x}_{k-g+1}[1]) + i_{k-g+1} R_0 + \hat{x}_{k-g+1}[2] + \hat{x}_{k-g+1}[3] \end{bmatrix} \quad (30)$$

where g is the innovation length.

Correspondingly, expand the KF gain K_k to a gain matrix $K_{g,k}$.

$$K_{g,k} = [K_k \quad K_{k-1} \quad \cdots \quad K_{k-g+1}] \quad (31)$$

Then replacing the single innovation e_k and the gain K_k in the state estimation equation $\hat{x}_k = \hat{x}_{k,k-1} + K_k e_k$ with the innovation vector $E_{g,k}$ and the gain matrix $K_{g,k}$ gives the optimized state:

$$x_k = \hat{x}_{k,k-1} + K_{g,k} E_{g,k} = \hat{x}_{k,k-1} + \sum_{j=0}^{g-1} K_{k-j+1} e(k-j) \quad (j = 1, 2, \dots, g-1) \quad (32)$$

In the equation $\hat{x}_k = \hat{x}_{k,k-1} + K_k e_k$, the state corrected term $K_k e_k$ is obtained by K_k multiplying a single innovation e_k . Through expanding e_k to $E_{g,k}$ and K_k to $K_{g,k}$, the optimized state $\hat{x}_k = \hat{x}_{k,k-1} + K_{g,k} E_{g,k}$ is achieved, and the term $K_{g,k} E_{g,k}$ is obtained by $K_{g,k}$ multiplying an innovation vector $E_{g,k}$ (i.e., multi-innovations). The innovation vector $E_{g,k}$ contains multiple innovations (more error corrected information); thus the multi-innovation EKF algorithm is more accurate than the EKF algorithm in SOC estimation.

Summarizing the above derivation yields the multi-innovation EKF (MI-EKF) algorithm as follows:

$$\hat{x}_{k,k-1} = \begin{bmatrix} 1 & 0 & 0 \\ 0 & e^{-T/\tau_1} & 0 \\ 0 & 0 & e^{-T/\tau_2} \end{bmatrix} \times \hat{x}_{k-1} + \begin{bmatrix} -\eta Ts/C_N \\ R_1(1-e^{-T/\tau_1}) \\ R_2(1-e^{-T/\tau_2}) \end{bmatrix} \times i_{k-1} \quad (33)$$

$$P_{k,k-1} = A_k P_{k-1} A_k^T + L_k Q_{k-1} L_k^T \quad (34)$$

$$K_k = \frac{P_{k,k-1} H_k^T}{H_k P_{k,k-1} H_k^T + M_k R_k M_k^T} \quad (35)$$

Table 3 Cyclic intermittent discharge experiment with different discharge rates.

Discharge rate	Current value (A)	Discharge completion time	Discharge stage setting	Experiment time
0.5C	1.45	2 h	Discharge the battery for 10 min and left it for 30 min	8 h
1C	2.9	1 h	Discharge the battery for 5 min and left it for 30 min	7 h
2C	5.8	0.5 h	Discharge the battery for 2.5 min and left it for 30 min	6.5 h

Table 4 The OCV and SOC relation.

SOC	1.0000	0.9167	0.8333	0.7500	0.6667	0.5833	0.5000	0.4167	0.3334	0.2500	0.1667	0.0834	0.0050
OCV (0.5C)	4.1328	4.0014	3.9995	3.8430	3.7286	3.5971	3.4068	3.3147	3.1761	3.0081	2.8276	2.6329	2.5542
OCV (1C)	4.0997	4.0209	3.9071	3.7940	3.6749	3.5491	3.4195	3.2840	3.1364	2.9687	2.7842	2.5762	2.5000
OCV (2C)	4.1176	3.9670	3.8510	3.7397	3.6232	3.5007	3.3742	3.2418	3.0961	2.9299	2.7461	2.5511	2.5003

$$e_k = U_k - U_{OC,k}(\hat{x}_k[1]) + i_k R_0 + \hat{x}_k[2] + \hat{x}_k[3] \tag{36}$$

$$E_{g,k} = \begin{bmatrix} e_k \\ e_{k-1} \\ \vdots \\ e_{k-g+1} \end{bmatrix}$$

$$= \begin{bmatrix} U_k - U_{OC,k}(\hat{x}_k[1]) + i_k R_0 + \hat{x}_k[2] + \hat{x}_k[3] \\ U_{k-1} - U_{OC,k-1}(\hat{x}_{k-1}[1]) + i_{k-1} R_0 + \hat{x}_{k-1}[2] + \hat{x}_{k-1}[3] \\ \vdots \\ U_{k-g+1} - U_{OC,k-g+1}(\hat{x}_{k-g+1}[1]) + i_{k-g+1} R_0 + \hat{x}_{k-g+1}[2] + \hat{x}_{k-g+1}[3] \end{bmatrix} \tag{37}$$

$$K_{g,k} = [K_k \quad K_{k-1} \quad \cdots \quad K_{k-g+1}] \tag{38}$$

$$\hat{x}_k = \hat{x}_{k,k-1} + K_{g,k} E_{g,k} \tag{39}$$

$$P_k = [I - K_k H_k] P_{k,k-1} \tag{40}$$

The steps of the MI-EKF algorithm in eqs. (33)–(40) are listed as follows:

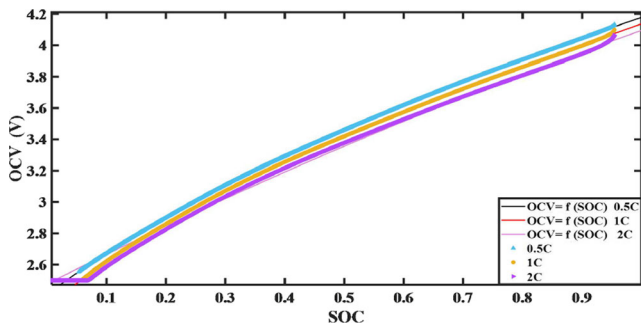


Fig. 5 The OCV-SOC curve of the battery

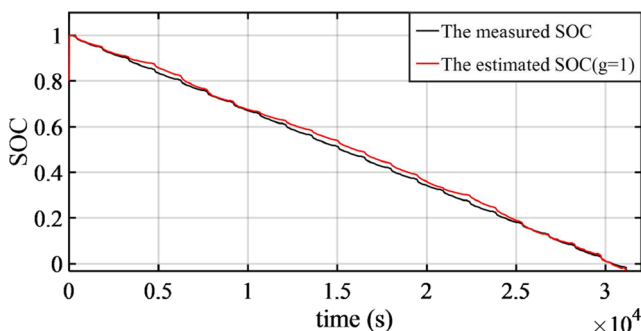


Fig. 6 The estimated/measured SOC by the EKF and the AH methods

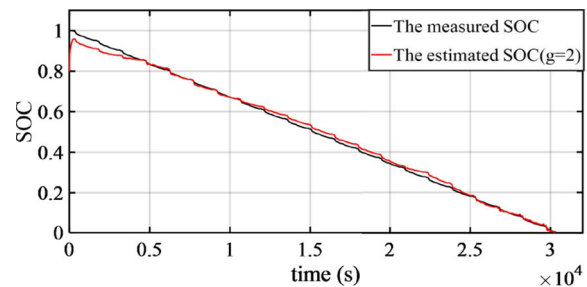
Experiment and simulation

The battery test platform

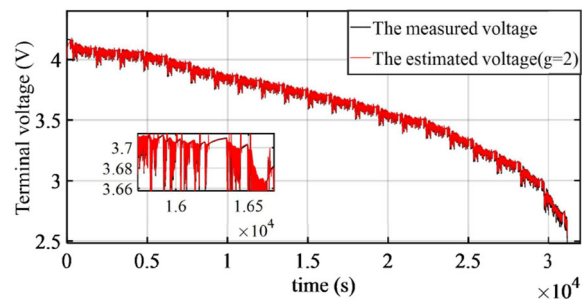
Referring to Fig. 3, take an actual battery charging and discharging system as an example. Its configuration diagram is displayed in Fig. 4. The battery experiment platform includes a battery tester (NEWARE BTS-4008-5V12A-TB), a median machine, a battery holder, 18,650 (2900 mAh) lithium batteries, and a host computer. The battery specifications are shown in Table 2.

The OCV-SOC relation

The OCV-SOC curve is obtained through a battery static test. The battery static test refers to a method of measuring the OCV in a stable state after stopping charging and discharging



(a) The estimated/measured SOC by the MI-EFK ($g=2$) and the AH methods.



(b) The estimated/measured terminal voltage by the MI-EFK ($g=2$) and the AH methods.

Fig. 7 The SOC/terminal voltage estimation by the MI-EFK ($g=2$) and the AH methods

for a period of time. The length of the static time determines the accuracy of the OCV measurement.

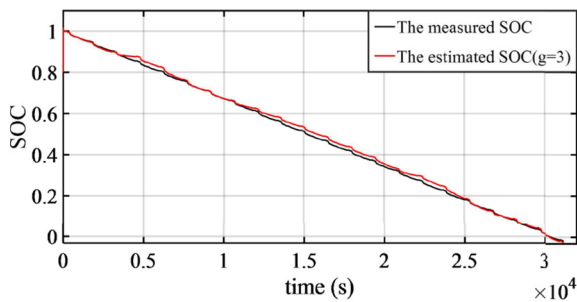
The principles of the static experiment are as follows:

- 1) The SOC measurement: the SOC of the battery is unable to get by direct measurement, so the principle of the AH integration method is used for computing SOC.
- 2) The OCV measurement: it can be seen from the eq. (1) (i.e., $U_k = U_{OC,k}(SOC_k) - I_k R_0 - U_k^{R_1} C_1 - U_k^{R_2} C_2$) that during the battery discharging, if the current is turned off and rests for a period of time, the voltages across R_0 , R_1 , and R_2 become zero as the discharging ends, and the terminal voltage measured at this time can be used as the OCV value.

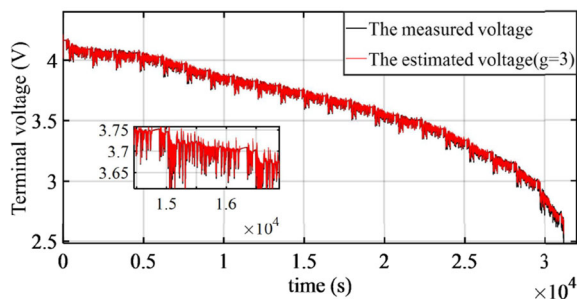
The steps of the static experiment are as follows:

1. Use different constant current to fully charge the battery for 2 h, and left it for 60 min.
2. The discharge experiment process is shown in Table 3, the sampled data is shown in Table 4.

By using the MATLAB curve fitting toolbox to fit the data of the OCV and SOC calculated by the AH

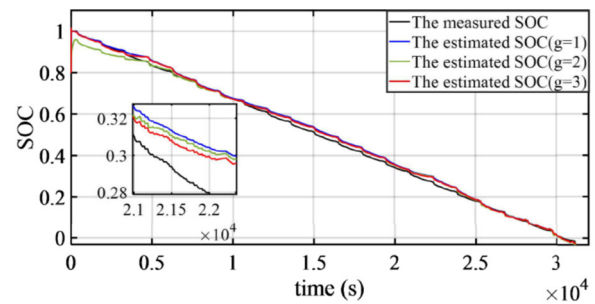


(a) The estimated/measured SOC by the MI-EFK ($g=3$) and the AH methods.

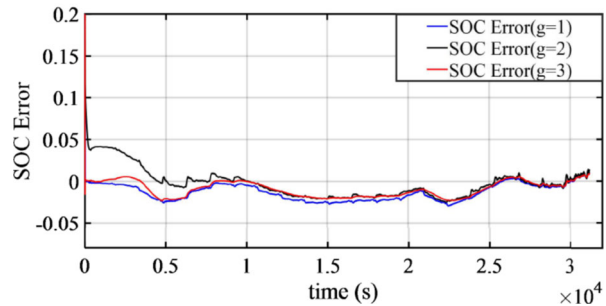


(b) The estimated/measured terminal voltage by the MI-EFK ($g=3$) and the AH methods.

Fig. 8 The SOC/terminal voltage estimation by the MI-EFK ($g=3$) and the AH methods



(a) The estimated/measured SOC by the MI-EFK (different g) and the AH methods.



(b) The error between the estimated/measured SOC under different g .

Fig. 9 Comparison of the SOC estimation by the MI-EFK algorithm under different g

integration method, the OCV-SOC curve is obtained, referring to Fig. 5. The static experiment shows that the OCV measurement accuracy can be improved under the smaller discharge current.

Considering the actual use of lithium batteries in electric vehicles, the lithium battery discharge experimental data is sampled under urban dynamometer driving schedule (UDDS) conditions. Apply the AH method, the EKF technique, and the explored MI-EKF technique to compute SOC based on MATLAB simulation. The simulation results are displayed in Figs. 6, 7, 8, and 9; for the convenience of observation, a partial enlargement map is drawn in the graph.

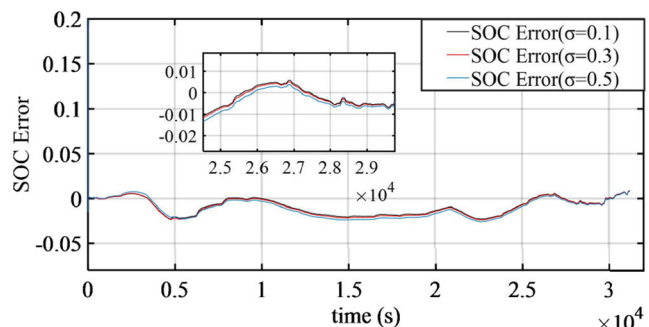


Fig. 10 SOC estimation error under different σ values

Figure 6 displays the estimated SOC of the EKF (i.e., the MI-EKF, $g = 1$) algorithm and the AH method.

Figure 7 displays the SOC and terminal voltage computed by the MI-EKF algorithm ($g = 2$) and the AH method.

Figure 8 displays the SOC and terminal voltage computed by the MI-EKF algorithm ($g = 3$) and the AH method.

Figure 9 displays the SOC computed by the MI-EKF algorithm under different g and the AH method, and displays the SOC error of the MI-EKF algorithm and the AH method.

From Fig. 6, 7, 8, and 9, we can get that the SOC estimation error by using the EKF algorithm (i.e., the MI-EKF $g = 1$) is much larger than the SOC estimation error by using the MI-EKF algorithm ($g = 2$ and $g = 3$). Generally, when taking the innovation length $g = 3$ in the MI-EKF algorithm, the estimated SOC is the most accurate and the SOC error is the smallest.

Noise influence on SOC estimates

The MI-EKF algorithm is unbiased estimation method under random noises corruption, especially under white noise corruption, but the SOC estimation accuracy varies under different variances.

Add an uncorrelated white noise sequence $\{v(t)\}$ with zero mean and variance $\sigma^2 = 0.1^2, 0.3^2, 0.5^2$, respectively. The SOC estimation errors under different σ^2 by using the MI-EKF algorithm are shown in Fig. 10. The following can be seen from the figure:

- 1) The parameter estimation errors given by the MI-EKF algorithm are generally smaller and approach zero which shows the effectiveness of the proposed algorithms.
- 2) The estimated SOC errors change small under different white noises. Generally, the estimated SOC errors by the MI-EKF algorithm are close to the true SOC as the noise variance becomes small.

Conclusion

According to the characteristics of lithium battery, an equivalent battery circuit is adopted and further a nonlinear state space equation is constructed. Through the linearization of the nonlinear battery equation, the EKF technique and the MI-EKF technique are carried out and are compared with the AH method. The experiment results prove that the MI-EKF algorithm can compute the SOC of the lithium battery more accurate and effective than that of the EKF algorithm, and as the innovation length increasing, the errors of the estimated SOC get smaller and smaller. Adding an uncorrelated white noise can slightly influence the SOC estimation error which will be small under small noise.

Due to the increase of the matrix dimension, the computation load of the MI-EKF algorithm is larger compared with that of the standard EKF algorithm, but the calculation precision of the MI-EKF algorithm is much improved compared with that of the EKF algorithm. The proposed method can be extended to study remaining useful life prediction for supercapacitors in Refs. [69, 70], and can apply to model block-oriented dynamic systems in Refs. [71–73].

Funding information This work was supported by the National Natural Science Foundation of China under Grant Nos. 61873138.

References

1. Zhou ZK, Kang YZ, Shang YL, Cui NX, Zhang CH, Duan B (2019) Peak power prediction for series-connected LiNCM battery pack based on representative cells. *J Clean Prod* 230:1061–1073
2. Duan B, Li ZYQ, Gu PW, Zhou ZK, Zhang CH (2018) Evaluation of battery inconsistency based on information entropy. *Journal of Energy Storage* 16:160–166
3. Lyu PZ, Liu XJ, Qu J, Zhao JT, Huo YT, Qu ZG, Rao ZH (2020) Recent advances of thermal safety of lithium ion battery for energy storage. *Energy Storage Mater* 31:195–220. <https://doi.org/10.1016/j.ensm.2020.06.042>
4. Feng L, Ding J, Han YY (2020) Improved sliding mode based EKF for the SOC estimation of lithium-ion batteries. *Ionics* 26:2875–2882
5. Xia B, Chen C, Tian Y, Wang M, Sun W, Xu Z (2015) State of charge estimation of lithium-ion batteries based on an improved parameter identification method. *Energy* 90:1426–1434
6. Panchal S, Mathew M, Dincer I, Agelin-Chaab M, Frase R, Fowler M (2018) Thermal and electrical performance assessments of lithium-ion battery modules for an electric vehicle under actual drive cycles. *Electr Power Syst Res* 163:18–27
7. Duan B, Zhang Q, Geng F, Zhang C (2019) Remaining useful life prediction of lithium-ion battery based on extended Kalman particle filter. *Int J Energy Res* 44:1724–1734
8. Zhu R, Duan B, Zhang C, Gong S (2019) Accurate lithium-ion battery modeling with inverse repeat binary sequence for electric vehicle applications. *Appl Energy* 251:113339
9. Ng K, Moo C, Chen Y, Hsieh Y (2009) Enhanced coulomb counting method for estimating state-of-charge and state-of-health of lithium-ion batteries. *Appl Energy* 86:1506–1511
10. Piller S, Perrin M, Jossen A (2001) Methods for state-of-charge determination and their applications. *J Power Sources* 96:113–120
11. Pei L, Zhu C, Lu R (2013) Relaxation model of the open-circuit voltage for state-of-charge estimation in lithium-ion batteries. *IET Elect Syst Transp* 3:112–117
12. Zhang Q, Cui N, Li Y, Duan B, Zhang C (2020) Fractional calculus based modeling of open circuit voltage of lithium-ion batteries for electric vehicles. *J Energy Storage* 27:100945
13. Hu L, Hu XS, Che Y, Feng F, Lin X, Zhang Z (2020) Reliable state of charge estimation of battery packs using fuzzy adaptive federated filtering. *Appl Energy* 262:114569
14. Çeven S, Albayrak A, Bayır R (2020) Real-time range estimation in electric vehicles using fuzzy logic classifier. *Comput Electr Eng* 83:106577
15. Hannan M, Lipu M, Hussain A, Saad M, Ayob A (2018) Neural network approach for estimating state of charge of lithium-ion

- battery using backtracking search algorithm. *IEEE Access* 6: 10069–10079
16. Chaoui H, Ibe-Ekeocha CC (2017) State of charge and state of health estimation for lithium batteries using recurrent neural networks. *IEEE Trans Veh Technol* 66(10):8773–8783
 17. Jiao M, Wang D, Qiu J (2020) A GRU-RNN based momentum optimized algorithm for SOC estimation. *J Power Sources* 459: 228051
 18. Hansen T, Wang C (2005) Support vector based battery state of charge estimator. *J Power Sources* 141:351–358
 19. Liu S, Wang J, Liu Q, Tang J, Liu H, Fang Z (2019) Deep-discharging li-ion battery state of charge estimation using a partial adaptive forgetting factors least square method. *IEEE Access* 7: 47339–47352
 20. Shrivastava P, Soon T, Idris M, Mekhilef S (2019) Overview of model-based online state-of-charge estimation using Kalman filter family for lithium-ion batteries. *Renew Sust Energ Rev* 113:109233
 21. Liu Z, Dang X, Jing B, Ji J (2019) A novel model-based state of charge estimation for lithium-ion battery using adaptive robust iterative cubature Kalman filter. *Electr Power Syst Res* 177:105951
 22. Chen M, Bai F, Song W, Lv J, Lin S, Feng Z, Li Y, Ding Y (2017) A multilayer electro-thermal model of pouch battery during normal discharge and internal short circuit process. *Appl Therm Eng* 120: 506–516
 23. Kim M, Chun H, Kim J, Kim K, Yu J, Kim T, Han S (2019) Data-efficient parameter identification of electrochemical lithium-ion battery model using deep Bayesian harmony search. *Appl Energy* 254:113644
 24. Guo F, Hu G, Zhou P, Huang T, Chen X, Ye M, He J (2019) The equivalent circuit battery model parameter sensitivity analysis for lithium-ion batteries by Monte Carlo simulation. *Int J Energy Res* 43:9013–9024
 25. Xuan D, Shi Z, Chen J, Zhang C, Wang Y (2020) Real-time estimation of state-of-charge in lithium-ion batteries using improved central difference transform method. *J Clean Prod* 252:119787
 26. Zhang W, Wang L, Wang L, Liao C (2018) An improved adaptive estimator for state-of-charge estimation of lithium-ion batteries. *J Power Sources* 402:422–433
 27. Grewal M, Andrews A (2002) *Kalman filtering: theory and practice using MATLAB*, Second edition. New York
 28. Mastali M, Vazquez-Arenas J, Fraser R, Fowler M, Afshar S, Stevens M (2013) Battery state of the charge estimation using Kalman filtering. *J Power Sources* 239:294–307
 29. Huang C, Wang Z, Zhao Z, Wang L, Lai C, Wang D (2018) Robustness evaluation of extended and unscented Kalman filter for battery state of charge estimation. *IEEE Access* 6:27617–27628
 30. Sepasi S, Ghorbani R, Liaw B (2014) Improved extended Kalman filter for state of charge estimation of battery pack. *J Power Sources* 255:368–376
 31. Guo L, Li J, Fu Z (2019) Lithium-ion battery SOC estimation and hardware-in-the-loop simulation based on EKF. *Energy Procedia* 158:2599–2604
 32. Dong X, Zhang C, Jiang J (2018) Evaluation of SOC estimation method based on EKF/AEKF under noise interference. *Energy Procedia* 152:520–525
 33. Plett G (2004) Extended Kalman filtering for battery management systems of LiPB-based HEV battery packs: part 3. *J Power Sources* 134:277–292
 34. Xiong R, He H, Sun F, Zhao K (2012) Evaluation on state of charge estimation of batteries with adaptive extended Kalman filter by experiment approach. *IEEE Trans Veh Technol* 62:108–117
 35. He H, Xiong R, Fan J (2011) Evaluation of lithium-ion battery equivalent circuit models for state of charge estimation by an experimental approach. *Energies* 4:582–598
 36. Van der Merwe R, Wan E (2001) The square-root unscented Kalman filter for state and parameter-estimation. *ICASSP* 6: 3461–3464
 37. Li Y, Wang C, Gong J (2017) A multi-model probability SOC fusion estimation approach using an improved adaptive unscented Kalman filter technique. *Energy* 141:1402–1415
 38. Liu G, Xu C, Jiang K, Wang K (2019) State of charge and model parameters estimation of liquid metal batteries based on adaptive unscented Kalman filter. *Energy Procedia* 158:4477–4482
 39. Wang R, Feng H (2020) Lithium-ion batteries remaining useful life prediction using wiener process and unscented particle filter. *Journal of Power Electronics* 20:270–278
 40. He W, Williard N, Chen C, Pecht M (2013) State of charge estimation for electric vehicle batteries using unscented Kalman filtering. *Microelectron Reliab* 53:840–847
 41. Arasaratnam I, Haykin S, Hurd R (2010) Cubature Kalman filtering for continuous-discrete systems: theory and simulations. *IEEE Trans Signal Process* 58:4977–4993
 42. Xu W, Xu J, Yan X (2020) Lithium-ion battery state of charge and parameters joint estimation using cubature Kalman filter and particle filter. *J Power Electron* 20:292–307
 43. Chen L, Xu L, Wang R (2017) State of charge estimation for lithium-ion battery by using dual square root cubature Kalman filter. *Math Probl Eng* 4:1–10
 44. Zeng Z, Tian J, Li D, Tian Y (2018) An online state of charge estimation algorithm for lithium-ion batteries using an improved adaptive cubature Kalman filter. *Energies* 11:1–16
 45. Arasaratnam I, Haykin S (2009) Cubature kalman filters. *IEEE Trans Autom Control* 54:1254–1269
 46. Bhuvana V, Unterrieder C, Huemer M (2013) Battery internal state estimation: a comparative study of non-linear state estimation algorithms. *IEEE Veh Power Propul Conf* <https://doi.org/10.1109/VPPC.2013.6671666>
 47. Xia B, Wang H, Tian Y, Wang M, Sun W, Xu Z (2015) State of charge estimation of lithium-ion batteries using an adaptive cubature Kalman filter. *Energies* 8:5916–5936
 48. Huang J, Wang Y, Wang Z, Han F, Li L (2014) The experiments of dual Kalman filter in lithium battery SOC estimation. *Appl Mech Mater* 494-495:1509–1512
 49. Tran N, Khan A, Choi W (2017) State of charge and state of health estimation of AGM VRLA batteries by employing a dual extended Kalman filter and an ARX model for online parameter estimation. *Energies* 10:10010137
 50. Propp K, Auger D, Fotouhi A, Marinescu M, Knap V, Longo S (2019) Improved state of charge estimation for lithium-sulfur batteries. *Journal of Energy Storage* 26:100943
 51. Wassiliadis N, Adermann J, Frericks A, Pak M, Reiter C, Lohmann B, Lienkamp M (2018) Revisiting the dual extended Kalman filter for battery state-of-charge and state-of-health estimation: A use-case life cycle analysis. *Journal of Energy Storage* 19:73–87
 52. Wei Z, Zou C, Leng F, Soong B, Tseng K (2018) Online model identification and state-of-charge estimate for lithium-ion battery with a recursive total least squares-based observer. *IEEE Trans Ind Electron* 65:1336–1346
 53. Wei Z, Zhao J, Xiong R, Dong G, Pou J, Tseng K (2019) Online estimation of power capacity with noise effect attenuation for lithium-ion battery. *IEEE Trans Ind Electron* 66:5724–5735
 54. Li Y, Chen J, Lan F (2020) Enhanced online model identification and state of charge estimation for lithium-ion battery under noise corrupted measurements by bias compensation recursive least squares. *J Power Sources* 456:227984
 55. Wang L, He Y (2019) Recursive least squares parameter estimation algorithms for a class of nonlinear stochastic systems with colored noise based on the auxiliary model and data filtering. *IEEE Access* 7:181295–181304

56. Zhang K, Ma J, Zhao X, Zhang D, He Y (2019) State of charge estimation for lithium battery based on adaptively weighting cubature particle filter. *IEEE Access* 7:166657–166666
57. He H, Xiong R, Zhang X, Sun F, Fan J (2011) State-of-charge estimation of the Lithium-ion battery using an adaptive extended Kalman filter based on an improved Thevenin model. *IEEE Trans Veh Technol* 60:1461–1469
58. Ding F, Chen T (2007) Performance analysis of multi-innovation gradient type identification methods. *Automatic* 43:1–14
59. Wang DQ, Ding F, Liu P (2009) Multi-innovation stochastic gradient algorithm for output error systems based on the auxiliary model. *Am Control Conf* <https://doi.org/10.1109/ACC.2009.5159814>
60. Liu Y, Yu L, Ding F (2010) Multi-innovation extended stochastic gradient algorithm and its performance analysis. *Circuits Syst Signal Process* 29:649–667
61. Ding F, Wang X ML, Xu L (2017) Joint state and multi-innovation parameter estimation for time-delay linear systems and its convergence based on the Kalman filtering. *Digit Signal Process* 62:211–223
62. Brand J, Zhang Z, Agarwal R (2014) Extraction of battery parameters of the equivalent circuit model using a multi-objective genetic algorithm. *J Power Sources* 247:729–737
63. Widanage W, Barai A, Chouchelamane G, Uddin K, McGordon A, Marco J, Jennings P (2016) Design and use of multisine signals for Li-ion battery equivalent circuit modelling, part 2: model estimation. *J Power Sources* 324:61–69
64. Kuo T, Lee K, Huang C, Chen J, Chiu W, Huang C, Wu S (2016) State of charge modeling of lithium-ion batteries using dual exponential functions. *J Power Sources* 315:331–338
65. Wang DQ, Mao L, Ding F (2017) Recasted models based hierarchical extended stochastic gradient method for MIMO nonlinear systems. *IET Control Theory Appl* 11(4):476–485
66. Chen J, Zhu QM, Liu YJ (2020) Modified Kalman filtering based multi-step-length gradient iterative algorithm for ARX models with random missing outputs. *Automatica*, 118 (2020). DOI: <https://doi.org/10.1016/j.automatica.2020.109034>
67. Chen J, Zhu QM, Ding F, Liu YJ (2020) Interval error correction auxiliary model based gradient iterative algorithms for multi-rate ARX models. *IEEE Trans Autom Control* DOI: <https://doi.org/10.1109/TAC.2019.2955030>
68. Chen GY, Gan M, Chen CLP, Li HX (2019) A regularized variable projection algorithm for separable nonlinear least squares problems. *IEEE Trans Autom Control* 64(2):526–537
69. Zhou YT, Wang Y, Wang K, Kang L, Peng F, Wang L, Pang J (2020) Hybrid genetic algorithm method for efficient and robust evaluation of remaining useful life of supercapacitors. *Appl Energy* 260:114169
70. Zhou YT, Huang Y, Pang J, Wang K (2019) Remaining useful life prediction for supercapacitor based on long short-term memory neural network. *J Power Sources* 440:227149
71. Wang DQ, Zhang S, Gan M, Qiu J (2020) A novel EM identification method for Hammerstein systems with missing output data. *IEEE Trans Ind Inform* 16:2500–2508
72. Wang DQ, Li L, Ji Y, Yan Y (2018) Model recovery for Hammerstein systems using the auxiliary model based orthogonal matching pursuit method. *Appl Math Model* 54:537–550
73. Wang DQ, Yan Y, Liu Y, Ding J (2019) Model recovery for Hammerstein systems using the hierarchical orthogonal matching pursuit method. *J Comput Appl Math* 345:135–145

Publisher's note Springer Nature remains neutral with regard to jurisdictional claims in published maps and institutional affiliations.